Determination of Maximum Mechanical Energy Efficiency in Energy Galloping Systems

J. Meseguer[1]; A. Sanz-Andrés[2]; and G. Alonso[3]

Abstract: Transverse galloping is a type of aeroelastic instability characterized by large amplitude, low frequency, normal to wind oscillations that appear in some elastic two-dimensional bluff bodies when subjected to a fluid flow, provided that the flow velocity exceeds a threshold critical value. Such an oscillatory motion is explained because of the energy transfer from the flow to the two-dimensional bluff body. The amount of energy that can be extracted depends on the cross section of the galloping prism. Assuming that the Glauert-Den Hartog quasi-static criterion for galloping instability is satisfied in a first approximation, the suitability of a given cross section for energy harvesting is evaluated by analyzing the lateral aerodynamic force coefficient, fitting a function with a power series in $\tan\alpha$ (α being the angle of attack) to available experimental data. In this paper, a fairly large number of simple prisms (triangle, ellipse, biconvex, and rhombus cross sections, as well as D-shaped bodies) is analyzed for suitability as energy harvesters. The influence of the fitting process in the energy harvesting efficiency evaluation is also demonstrated. The analysis shows that the more promising bodies are those with isosceles or approximate isosceles cross sections. **DOI: 10.1061/(ASCE)EM.1943-7889.0000817.**

Author keywords: Galloping; Energy harvesting; Wind tunnel.

Introduction

The potential use of different aeroelastic phenomena to extract energy from an incident flow, and through the oscillations of the excited structure, convert those oscillations into piezoelectric or electromagnetic energy, is receiving the attention of more and more researchers (St. Clair et al. 2010; Peng and Chen 2012). As a consequence, numerous studies have been published recently on the use of fluid-bodies instabilities interactions (the number of papers has remarkably grown in the last 2 years). The focus of these papers has been either on the particularities of oscillating systems (transverse galloping, wake galloping, flutter, and vortex shedding) or on the use of these oscillating systems for energy harvesting.

Besides the pioneer work of Glauert (1919), Den Hartog (1965), Novak (1969), Novak and Tanaka (1974), and Luo et al. (1988), among others, some relevant publications have appeared more recently concerning transverse galloping instability (Naudascher and Rockwell 1994; Luo et al. 1998; Barrero-Gil et al. 2010; Païdoussis et al. 2010, Sewatkar et al. 2012, Alonso and Meseguer 2014; Ibarra et al. 2014), whereas the use of transverse galloping for energy harvesting purposes has been analyzed by Sirohi and Mahadik (2011, 2012), Abdelkefi et al. (2012a, 2013a), Abdelkefi et al. (2013c, 2014), and Zhao et al. (2012).

However, transverse galloping is not the only flow-induced oscillating phenomenon in energy harvesting devices, and some efforts have been devoted to using other instability sources, such as wake galloping (Jung et al. 2009; Akaydin et al. 2010; Jung and Lee 2011; Abdelkefi et al. 2013b, c), vortex-induced vibrations (Abdelkefi et al. 2012b; Grouthier et al. 2012; Hobbs and Hu 2012; Peng and Chen 2012; Mackowski and Williamson 2013; Mehmood et al. 2013), and flutter of streamlined bodies (Peng and Zhu 2009; Tang et al. 2009; Zhu et al. 2009; Erturk et al. 2010; Bryant et al. 2011; Doaré and Michelin 2011; Zhu 2011; Abdelkefi et al. 2012c, d; Abdelkefi and Nuhait 2013; Bae and Inman 2014).

Most of these studies focused on the analysis of the suitability of some specific mechanisms to efficiently harvest the energy through different energy converters (piezoelectric, electromagnetic, etc.). In contrast, some attempts have been made to develop methodologies to evaluate the energy harvesting efficiency of two-dimensional bluff bodies from a purely aeroelastic point of view.

In this sense, Barrero-Gil et al. (2010) developed a simple approach to evaluate the efficiency of the transverse galloping of bluff bodies as an energy harvesting mechanism. To do this, following an already published methodology (Ng et al. 2005), a first approximation of the transverse galloping phenomenon can be explained by a one-degree of freedom (the transverse displacement, z) linear differential equation. The forcing aerodynamic coefficient c_z is expanded in a power series of the transverse velocity, $\mathrm{d}z/\mathrm{d}t$, retaining for simplicity only, the two first terms in the c_z series expansion, that is, $c_z = a_1(\mathrm{d}z/\mathrm{d}t)/U + a_3[(\mathrm{d}z/\mathrm{d}t)/U]^3$. Barrero-Gil et al. (2010) demonstrates that, within this approximation, the maximum harvesting efficiency is $\eta_{\max} = -a_1^2/(6a_3)$. The criterion developed is applied to assess the energy harvesting efficiency of several two-dimensional bodies (square, isosceles triangle, and D-section) whose aerodynamic coefficients are taken from the existing literature. The conclusion drawn is that D-shaped, two-dimensional bodies are the most appropriate ones for energy harvesting devices based on transverse galloping, because they provide the highest $\eta_{\max}$ value among the considered bodies.

Further experiments conducted at IDR/UPM on families of bodies with different cross sections provided a better insight on the transverse galloping phenomenon, and allowed for improvement of the approach initiated by Barrero-Gil et al. (2010) to predict the

[1]Professor, IDR/UPM, E.T.S.I. Aeronáuticos, Univ. Politécnica de Madrid, E-28040 Madrid, Spain. E-mail: j.meseguer@upm.es

[2]Professor, IDR/UPM, E.T.S.I. Aeronáuticos, Univ. Politécnica de Madrid, E-28040 Madrid, Spain. E-mail: angel.sanz.andres@upm.es

[3]Professor, IDR/UPM, E.T.S.I. Aeronáuticos, Univ. Politécnica de Madrid, E-28040 Madrid, Spain (corresponding author). E-mail: gustavo.alonso@upm.es

Note. This manuscript was submitted on May 20, 2013; approved on May 2, 2014; published online on ■■■■■■. Discussion period open until ■■■■■■■■■■■■■■■■■■; separate discussions must be submitted for individual papers. This paper is part of the ***Journal of Engineering Mechanics***, © ASCE, ISSN 0733-9399/040■■■■■(8)/$25.00.

energy harvesting efficiency of these structures by also providing a larger set of experimental aerodynamic data to validate the methodology. In particular, the transverse galloping stability of triangles (Alonso et al. 2005, 2007; Alonso and Meseguer 2006), ellipses (Alonso et al. 2010), biconvex, and rhombi (Alonso et al. 2009) were thoroughly determined by wind tunnel testing of cylinders with respective cross-sectional geometry and variable relative thickness.

By properly using the new and extended set of experimental aerodynamic data, it is possible to further develop and improve the methodology presented in Barrero-Gil et al. (2010) to evaluate the transverse galloping energy efficiency of bluff bodies.

A brief summary of the theoretical foundation already published in Barrero-Gil et al. (2010) is provided in the "Mathematical Model" section, and a new and improved way to estimate η_{max} is presented. The section "Analysis of the Energy Harvesting Properties of Several Bluff Bodies" is devoted to the application of the η_{max} criterion to a large amount of new cross-sectional shapes. Conclusions are outlined in the "Conclusions" section.

Mathematical Model

Theoretical foundations of galloping are well established and understood (Den Hartog 1965; Novak 1969, 1972). The simplest model to analyze the translational galloping behavior of a bluff body consists of a damped spring-mounted cylindrical body under the action of an incoming smooth flow of velocity U, parallel to the x-axis (Fig. 1). Other relevant magnitudes are the cylinder mass per unit length, m, the mechanical damping ratio, ζ, the natural circular frequency of oscillations, ω_n, the fluid density, ρ, and a characteristic transversal length of the galloping two-dimensional body (as the normal to wind length of its cross section, b_m). Then, assuming the body is slender enough to assure two-dimensional flow, the dynamics of the system is driven by

$$m\left(\frac{d^2z}{dt^2}+2\zeta\omega_n\frac{dz}{dt}+\omega_n^2 z\right)=f_z(\alpha)=\frac{1}{2}\rho U^2 b_m c_z(\alpha) \qquad (1)$$

where z = vertical displacement; t = time; f_z = instantaneous two-dimensional lateral force (parallel to the z-axis); c_z = instantaneous two-dimensional lateral force coefficient; ω_n = undamped resonance frequency; and ζ = damping coefficient.

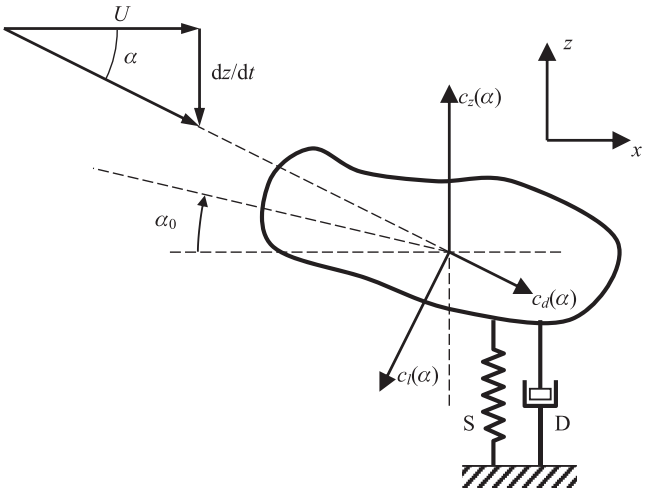

Fig. 1. Two-dimensional body in galloping oscillation: $c_l(\alpha)$, $c_d(\alpha)$, lift and drag coefficients, respectively; $c_z(\alpha)$, vertical force coefficient; D, damper; dz/dt, vertical velocity caused by galloping motion; S, spring; U, upstream unperturbed flow velocity; α, angle of attack, α_0, reference angle

In a body reference frame, across-wind oscillation of the structure periodically changes the angle of attack of the incident wind. Such a variation in the angle of attack produces variation in the aerodynamic forces acting on the structure (Fig. 1), which, in turn, affects the dynamic response of the structure. Therefore, transverse galloping can be explained as although the incident velocity U is uniform and constant, because of the lateral oscillation of the body, in a body reference system, the total velocity changes both its magnitude and direction with time. Consequently, the body angle of attack also changes with time, hence, the aerodynamic forces acting on it.

Consider that a structure at rest is oriented at a given angle of reference α_0 with respect to the incident flow (Alonso et al. 2005; Alonso and Meseguer 2006). When the body oscillates along the z-axis direction within an uniform flow with velocity U, the relative velocity between the fluid and the body is $U_r = \left[U^2+(dz/dt)^2\right]^{1/2} = U\left(1+\tan^2\alpha\right)^{1/2}$, where the angle of attack caused by the oscillation is $\tan\alpha = (dz/dt)/U$; therefore, $U_r = U/\cos\alpha$. Drag, $d(\alpha)$, and lift, $l(\alpha)$, forces are, respectively, $d(\alpha)=(1/2)\rho U_r^2 b_m c_d(\alpha)$ and $l(\alpha)=(1/2)\rho U_r^2 b_m c_l(\alpha)$, where $c_d(\alpha)$ stands for the drag coefficient, $c_l(\alpha)$ is the lift coefficient, ρ is the fluid density, and b_m is the characteristic transversal length of the cylinder, as already stated.

The projection of those forces in the z-axis direction is $f_z(\alpha) = -d(\alpha)\sin\alpha - l(\alpha)\cos\alpha$, and then Eq. (1) reads as

$$\begin{aligned} m\left(\frac{d^2z}{dt^2}+2\zeta\omega_n\frac{dz}{dt}+\omega_n^2 z\right) &= -\frac{1}{2}\rho U_r^2 b_m\left[c_d(\alpha)\sin\alpha + c_l(\alpha)\cos\alpha\right] \\ &= -\frac{1}{2}\rho U^2 b_m \frac{c_d(\alpha)\tan\alpha + c_l(\alpha)}{\cos\alpha} \\ &= \frac{1}{2}\rho U^2 b_m c_z(\alpha) \end{aligned} \qquad (2)$$

To solve Eq. (2), the function $c_z(\alpha)$ can be expanded in a power series of $\tan\alpha$ (Barrero-Gil et al. 2010; Ng et al. 2005) by fitting the function $c_z(\alpha)$, measured, for instance, in wind tunnel tests, to a polynomial in $\tan\alpha$ as

$$c_z(\alpha)=\sum_{j=1}^{\infty} a_{2j-1}\tan^{2j-1}\alpha \qquad (3)$$

Only the antisymmetric part of $c_z(\alpha)$ around $c_z(\alpha_0)$ contributes to galloping. Therefore, only the antisymmetric part of $c_z(\alpha)$ is used to obtain the polynomial Eq. (3). As long as α is small enough, the linear term coefficient α_1 reduces to the function $dc_l/d\alpha + c_d$ appearing in the Glauert-Den Hartog quasi-static criterion for galloping. Considering the movement is quasi-steady, because $\tan\alpha \ll 1$, the lateral force coefficient becomes $c_z(\alpha) \cong -(c_d\alpha + c_l) + O(\alpha^2) = -(c_d + dc_l/d\alpha)\alpha + O(\alpha^2)$; hence, $a_1 = -(c_d + dc_l/d\alpha)$.

The usual dimensionless variables in aeroelastic analysis are now introduced: $y = z/b_m$, $\tau = \omega_n t$, $m^* = m/(\rho b_m^2)$, and $U^* = U/(\omega_n b_m)$ in Eq. (2), and substituting $c_z(\alpha)$ by its series expansion in Eq. (3), Eq. (2) yields

$$\frac{d^2\psi}{d\tau^2}+2\zeta\frac{d\psi}{d\tau}+\psi=\frac{U^{*2}}{2m^*}\sum_{j=1}^{\infty}a_{2j-1}\left(\frac{1}{U^*}\frac{d\psi}{d\tau}\right)^{2j-1} \qquad (4)$$

where y = dimensionless vertical displacement; τ = dimensionless time; m^* = ratio of the mean density of the body to the density of the surrounding fluid; and U^* = reduced velocity.

Once the problem formulation has been established (the preceding differential equation with suitable boundary and initial conditions), an approximation to the problem solution can be

obtained by applying, for instance, the procedure already presented in Barrero-Gil et al. (2010). The method consists of the application of the Krylov-Bogoliubov method to this differential equation to obtain the time variation of the dimensionless galloping amplitude. To solve the problem, it is assumed that the body motion can be expressed as $\psi = A^*(\tau)\cos[\tau + \phi(\tau)]$, where $A^*(\tau)$ and $\phi(\tau)$ are functions slowly varying with τ. Then, the dimensionless amplitude becomes

$$\frac{dA^*}{d\tau} = -\frac{1}{2\pi}\int_0^{2\pi}\left[-2\zeta\frac{d\psi}{d\tau} + \frac{U^{*2}}{2m^*}\sum_{j=1}\frac{a_{2j-1}}{U^{*2j-1}}\left(\frac{d\psi}{d\tau}\right)^{2j-1}\right]\sin(\tau+\phi)d\tau$$
$$= \zeta A^* - \frac{U^{*2}}{4m^*}\left[a_1\frac{A^*}{U^*} + \frac{3}{4}a_3\left(\frac{A^*}{U^*}\right)^3 + \frac{5}{8}a_5\left(\frac{A^*}{U^*}\right)^5 + \frac{35}{64}a_7\left(\frac{A^*}{U^*}\right)^7 + \frac{63}{128}a_9\left(\frac{A^*}{U^*}\right)^9 + \cdots\right] \quad (5)$$

The steady amplitude of the oscillations is given by the real and positive roots of $dA^*/d\tau = 0$. Independent of the number of terms retained in Eq. (5), one of the roots is always $A^* = 0$. The analytical calculation of the other roots of Eq. (5) becomes more and more complicated as the number of terms increases. If only a_1 and a_3 are retained, the efficiency, or conversion factor, defined by the ratio of the power extracted by the structure from the flow per unit length and the total power in the flow per unit length, becomes $\eta_{max} = -a_1^2/(6a_3)$, as already stated.

The power that can be obtained in a cycle from transverse galloping oscillations, P_g, is obtained from the expression

$$P_g = \frac{1}{T}\int_0^T f_z\frac{dz}{dt}dt = \frac{\rho U^2 b}{2T}\int_0^T c_z\frac{dz}{dt}dt \quad (6)$$

where T = oscillation period.

In contrast, the power associated with the unperturbed flow is $P_f = \rho U^3 b_m/2$, and therefore, the energy harvesting efficiency is $\eta = P_g/P_f$.

The direct integration of Eq. (6), after the introduction of the dimensionless variables, to obtain P_g as performed in Barrero-Gil et al. (2010), results in a value for the efficiency of

$$\eta = \frac{1}{2}\left[a_1\left(\frac{A^*}{U^*}\right)^2 + \frac{3}{4}a_3\left(\frac{A^*}{U^*}\right)^4 + \frac{5}{8}a_5\left(\frac{A^*}{U^*}\right)^6 + \frac{35}{64}a_7\left(\frac{A^*}{U^*}\right)^8 + \frac{63}{128}a_9\left(\frac{A^*}{U^*}\right)^{10} + \cdots\right] \quad (7)$$

A different approach can be introduced here for the determination of the efficiency in a simpler way. The idea is to evaluate the power P_g, not the aerodynamic force used in Eq. (6), f_z, but the dissipative term in Eq. (1), that is, the left-hand side of Eq. (1). Eq. (6) for P_g then becomes

$$P_g = \frac{m}{T}\left[\int_0^T\frac{d^2z}{dt^2}\frac{dz}{dt}dt + 2\zeta\omega_n\int_0^T\left(\frac{dz}{dt}\right)^2dt + \omega_n^2\int_0^T z\frac{dz}{dt}dt\right]$$
$$= \frac{2m\zeta\omega_n}{T}\int_0^T\left(\frac{dz}{dt}\right)^2dt \quad (8)$$

In writing the last term of Eq. (8), it has been considered that, z being a periodic function, the integrals of both $(d^2z/dt^2)\times(dz/dt)$ and $z\times(dz/dt)$ are zero in a cycle.

Then, because it has been assumed that $z = A(t)\cos[\omega_n t + \phi(t)]$, and the introduction of the dimensionless variables already having been defined, gives $\psi = A^*(\tau)\cos[\tau + \phi(\tau)]$, and $dz/dt = \omega_n b_m d\psi/dt = -\omega_n b_m A^*\sin(\tau+\phi)$, where it has been considered that the time variation of both $A^*(\tau)$ and $\phi(\tau)$ is so slow that they can be considered constant in a cycle. Therefore

$$P_g = \zeta\frac{m\omega_n^3 b_m^2}{\pi}\int_0^{2\pi}\left(\frac{d\psi}{d\tau}\right)^2d\tau$$
$$= \zeta\frac{m\omega_n^3 b_m^2}{\pi}\int_0^{2\pi}\{-A^*(\tau)\sin[\tau+\phi(\tau)]\}^2d\tau = \zeta m\omega_n^3 b_m^2 A^{*2} \quad (9)$$

Thus, the expression giving the efficiency now results in

$$\eta = \frac{2\zeta m^*}{U^*}\left(\frac{A^*}{U^*}\right)^2 \quad (10)$$

where ζm^* is proportional to the Scruton number. Obviously, this last expression states that the only energy that is harvested out of the flow by the galloping motion is the energy dissipated by the structure.

The analytical calculation of the maximum efficiency becomes too complex when more than the first two terms in the polynomial approximation to $c_z(\alpha)$, Eq. (3), are considered. In that case, the problem solution is better achieved by a numerical method. The procedure used in the present work when more than two terms are used in Eq. (3) is the following:

1. First, the coefficients a_{2j-1} of the series expansion in Eq. (3) are calculated by fitting this expression to available experimental data. Note that the values of the fitted coefficients depend on the number of terms considered in Eq. (3).
2. Once the coefficients a_{2j-1} are known, the corresponding functions $dA^*/d\tau$, Eq. (5), are evaluated. It must be pointed out that the parameters involved in Eq. (5) are A^*, U^*, and ζm^*; therefore, in this process, two of them are fixed (namely, A^* and ζm^*), whereas the third one, U^*, is considered to be an independent variable. The result depends on the values chosen for A^* and ζm^* (additional comments on this point are given later in this work).
3. The roots of $dA^*/d\tau = 0$ are then calculated; thus, the critical values of U^* corresponding to the selected values of A^* and

ζm^* are obtained (formally, the smaller value of the critical U^* is the one of interest).

4. Then, the efficiency is determined by using either Eq. (7) or Eq. (10) as a function of U^*, A^*, and ζm^*.

Analysis of the Energy Harvesting Properties of Several Bluff Bodies

In the simplest approach, when only the first two terms (a_1 and a_3) are considered in the series (3), the maximum efficiency occurs when $\eta_{max} = -a_1^2/(6a_3)$. This expression gives a rough approximation to the quality of a given two-dimensional body to extract energy through transverse galloping oscillations. Despite the limited application of this approximation, it seems clear that the more promising bodies for power extraction are those whose cross sections provide large positive values of the coefficient a_1 and small negative values of a_3. In a first approximation (small values of the angle of attack), the coefficient a_1 can be identified with the Glauert-Den Hartog parameter for galloping, and it must be positive (the body must be stalled), whereas a_3 has to be negative, because this parameter represents the capacity of the system to keep the amplitude of the galloping oscillations between finite boundaries (limit cycle oscillations).

Note also that when only two terms are considered, the maximum efficiency does not depend on the parameters involved in Eq. (10). This expression is not applicable, however, when more terms are retained in Eq. (5).

Using sufficient terms in the series expansion of the force coefficient $c_z(\alpha)$ is important for properly predicting the energy harvesting efficiency of a given structure. In addition, when this force coefficient is obtained from experimental data, the process of fitting these data determines the accuracy of the results. The fitting process is affected by the value of the reference angle α_0 selected [formally, only the antisymmetric part of $c_z(\alpha)$ obtained from experimental data are considered] and by the number of data points taken around the central one. In the fitting process of a given equation to a set of experimental data, the first condition that should be fulfilled is that the equation must be appropriate to reproduce the main features of the experimental data (in the case of a power series, this is generally achieved by retaining enough terms in the truncated series), otherwise, very different conclusions can be reached from the conclusions that the experimental data show.

The main purpose of this work is to investigate how the approximation chosen to derive the force coefficient from the experimental data for calculating the energy harvesting efficiency determines the accuracy of the results. The criteria derived for that approximation, together with the simpler approach to evaluate the harvesting efficiency presented in the "Mathematical Model" section, substantially improves the method presented in Barrero-Gil et al. (2010). This improved method is applied to bodies with different cross sections.

The analysis is performed first on D-shaped cross sections, whose efficiency is derived in Barrero-Gil et al. (2010) by choosing a cubic polynomial for the force coefficient approximation from experimental data available in the literature. To contrast these results and apply the new findings to the energy harvesting efficiency evaluation, new wind tunnel tests were performed at IDR/UPM on a D-shaped cross-section body.

A prism with the cross section (Fig. 2) was built up, and its aerodynamic properties were measured in the A9 wind tunnel at IDR/UPM. This wind tunnel is an open circuit, closed test chamber whose cross section is 1.8-m high and 1.5-m wide. Turbulence intensity is approximately 2.5% at 20 m/s wind velocity. The model span was 0.8 m, and there were two flat plates parallel to the flow at

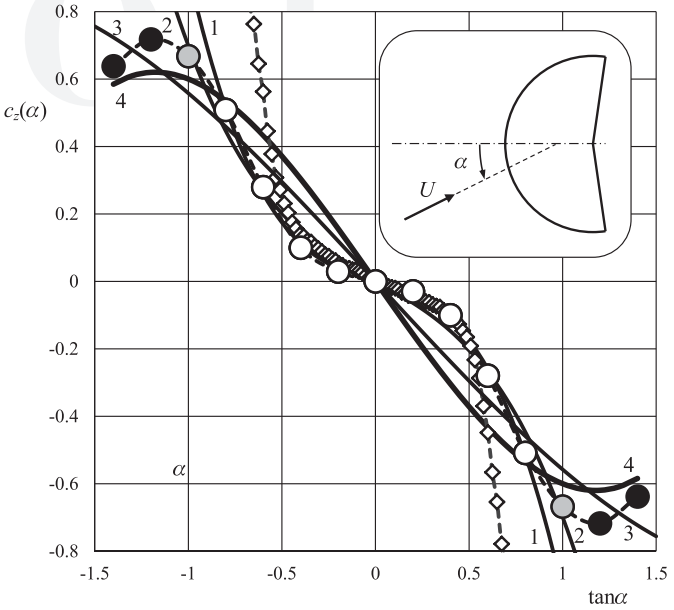

Fig. 2. Variation with tan α of the lateral force coefficient c_z in the case of D-shaped bodies (symbols and key lines are explained in the text)

the ends of the prism to assure two-dimensional behavior. Aerodynamic loads were measured through a six-component strain-gauge balance (ATI DELTA, ATI Industrial Automation, Apex, North Carolina), whereas the flow velocity was measured with a Pitot tube (model 3.3.311, Airflow Systems, Dallas, Texas), connected to a Schaewitz Lucas pressure transducer. The D-shaped model was mounted on a rotating platform NEWPORT RV120-PP-HL (Newport Corporation, Irvine, California), which, in turn, was mounted on the strain-gauge balance. The rotating platform can set the model angle of attack within $\pm 0.1°$ accuracy. The balance has a maximum measurement uncertainty of 1.25%. No provisions for blockage corrections of the measured loads have been undertaken, as even in the worst case, the model front area (including end plates) is less than 8% of the test section flow area.

Aerodynamic forces were measured from $\alpha_0 = -90°$ to $\alpha_0 = +90°$ at a 1° step. At each reference angle, the loads were sampled at 200 Hz during 30 s. The results obtained are shown in Fig. 2, in the same plot of the experimental data reported by Barrero-Gil et al. (2010). In Fig. 2, the symbols represent the experimental data reported by Barrero-Gil et al. (2010) (circles) and the data measured at IDR/UPM facilities (rhombi). The lines correspond to fitted equations in the experimental data reported by Barrero-Gil et al. (2010) (circles) by retaining only the first two terms in Eq. (3) (solid lines). The influence of the number of experimental points in the fitting process is as follows: line 1 represents the fitting result when only nine experimental points (white circles) are used; line 2 represents the fitting result when 11 experimental points (white and gray circles) are considered, and line 3 is obtained when the whole set of experimental points reported by Barrero-Gil et al. (2010) is considered in the fitting process [15 experimental points (white, gray, and black circles)]. Line 4 is the one given in Barrero-Gil et al. (2010), fitting with only two terms.

The dependence on the considered number of experimental points used to fit lateral force coefficients to data presented in Fig. 2 can be found in Table 1.

There are some differences between the two sets of experimental data, which can be explained by keeping in mind the experiments described herein, that the noncircular part of the D-shaped body

contour is not exactly a flat surface, but is formed by two planes, creating an angle of 170° between them (instead of 180°). This slightly modifies the aerodynamic behavior at large values of the angle of attack (in this case, the relative thickness is 1.84 instead of 2).

The force coefficient curve is then fitted by taking different numbers of experimental points measured during the IDR/UPM wind tunnel tests to assess the influence of this parameter, and thus, the fitting curves using the 9, 11, and 15 experimental points are also represented in Fig. 2. Finally, the fitting curve given in Barrero-Gil et al. (2010) is also included in Fig. 2. A close look at the curves in Fig. 2 indicates how important it is to have the right choice of the approximation to $c_z(\alpha)$ from the experimental data; specifically, if the range of experimental data points is large (this applies to D-shaped cross sections but also to other bodies), then the curvature variation of the function should not be so simple. As shown in Fig. 2, the real behavior of the experimental data is characterized by an almost zero slope at the origin, but if the data interval taken for the curve fitting is too large, the extreme points of the interval are those driving the value of the slope of the fitting curve. In this case, it is possible to obtain a fitting curve with a slope at the origin larger than that shown by the experimental data, which means an overestimation of the energy harvesting efficiency. The curvature of the curves at the origin is also changed.

The new approach for the evaluation of the energy harvesting efficiency is also applied to other two-dimensional bodies that may be unstable and experience transverse galloping oscillations. During the past several years, a research program devoted to studying the transverse galloping characteristics of prismatic bodies with simple basic cross-sectional shapes has been carried out at IDR/UPM. Within this program, parametric experimental studies of bodies like isosceles triangles, ellipses, biconvex aerofoils, and rhombi (Fig. 3) have been carried out by wind tunnel tests. The parameters that define the members of a given family of bluff bodies are the relative thickness, τ, which is defined as the ratio of the maximum thickness, b_m, of the reference body cross section to its chord, c. The reference body cross section is the one corresponding to $\alpha_0 = 0$ (Fig. 3). Similar $c_z(\alpha)$ curves for these bodies, as the one depicted in Fig. 2, can be found in Alonso and Meseguer (2006), in Alonso et al. (2005, 2007) in the case of triangular cross section bodies, in Alonso et al. (2009) for biconvex cross section bodies, in Alonso et al. (2009) and in Ibarra et al. (2014) for rhomboidal cross-section prisms, and in Alonso et al. (2010) for elliptical cross-section beams. In all the preceding cases, the dependence of $c_z(\alpha)$ on the parameters defining the section geometry is considered.

Obviously, to extract energy from galloping oscillations, the configuration must develop instability, which according to published information, only occurs at given values of the reference angle α_0, which is different for each family of bodies. The different stability maps for the previously listed geometries have been published elsewhere. Information concerning triangular prisms can be found in Alonso et al. (2005, 2007, 2012), Alonso and Meseguer (2006), and Iungo and Buresti (2009); elliptical bodies are considered in Alonso et al. (2010), and both biconvex and rhomboidal cross-section bodies are analyzed in Alonso et al. (2009).

The corresponding values of the function $c_z(\alpha) = [c_d(\alpha)\tan\alpha + c_l(\alpha)]/\cos\alpha$ have been calculated from the available wind tunnel tests data on the aerodynamic coefficients of the bodies under consideration. These data are fitted to polynomials in $\tan\alpha$, thus giving the values of the coefficients a_{2j-1}. Then, the maximum efficiencies are obtained according to Eq. (10) and the new approach presented in the "Mathematical Model" section.

The geometry that shows the maximum efficiency now needs to be determined, as well as which geometry (represented by its relative thickness) also shows the maximum efficiency for each family of bodies. Fig. 4 shows the variation with the relative thickness of the maximum efficiency of the different families of bluff bodies. The results represented in Fig. 4 correspond to the case $A^* = 2$ and $\zeta m^* = 1(\alpha_0 \cong 180°)$, but, as has already been mentioned, these results will be different if other values of the parameters concerned are considered. Such behavior is shown in Fig. 5, where the variation of the maximum efficiency with the dimensionless amplitude A^*, in the case of isosceles triangular bodies with main vertex angle $\beta = 30°$, is shown. There are two families of curves in this plot. Those that are almost vertical straight lines come from Eq. (7) for the giving values of U^*, whereas the curved lines are obtained from Eq. (10), assuming some fixed values of ζm^*.

From this plot, it can be realized that once U^* is fixed, the amplitude of oscillations A^* for maximum efficiency is fixed, because

Table 1. Variation of the a_1 and a_3 Coefficients Appearing in Eq. (3) of the Lateral Force Acting on D-shaped Bodies

Line number	Number of experimental points	a_1	a_3
1	11	−0.159	−0.758
2	9	−0.305	−0.394
3	15	−0.601	0.043
4	The same as line 3, but (0,0) excluded	−0.79	0.19

Note. $c_z(\alpha) = a_1\tan\alpha + a_3\tan^3\alpha$, as a function of the number of experimental points used to fit the previous expression to experimental data represented in Fig. 2. Line number identifies the fitting curve in Fig. 2. Line 4 corresponds to the results reported in Barrero-Gil et al. (2010).

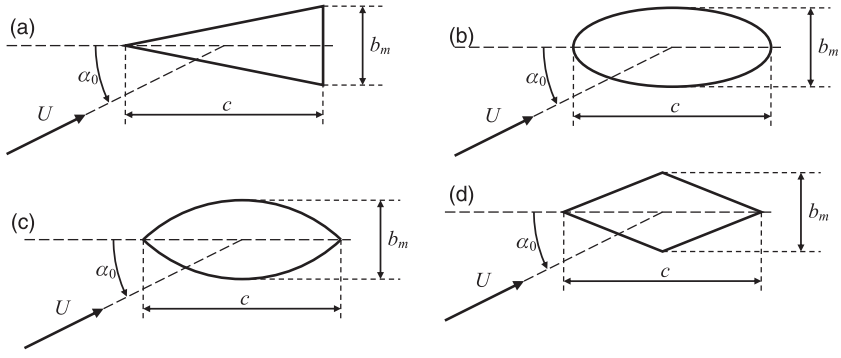

Fig. 3. Two-dimensional prism families whose energy harvesting suitability under galloping oscillations are considered: (a) triangle; (b) ellipse; (c) biconvex; (d) rhombus

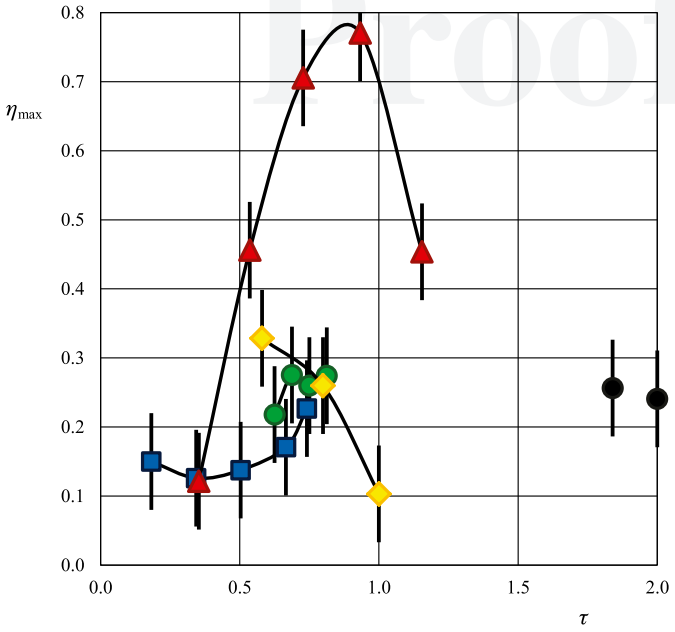

Fig. 4. Maximum efficiency, η_{max}, versus relative thickness, τ, of the different families of prisms shown in Fig. 3; triangles at $\alpha_0 \cong 180°$ (triangles); rhombi (rhombi), biconvex (squares), and ellipses (circles); solid circles represent results of D-shaped bodies; vertical bars indicate the estimated error

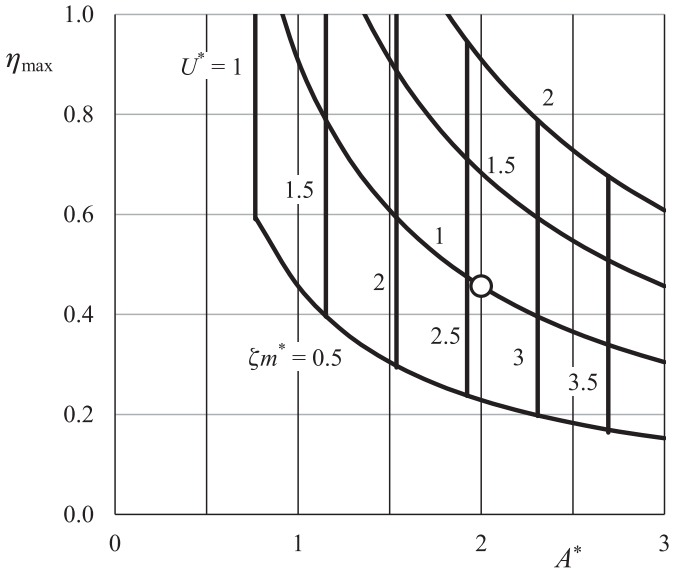

Fig. 5. Variation of the maximum efficiency for energy harvesting, η_{max}, with the dimensionless amplitude of galloping oscillations, A^*, of a two-dimensional bluff body whose cross section is an isosceles triangle with a main vertex $\beta = 30°$; results correspond to $\alpha_0 = 180°$; numbers on the curves indicate the values of the reduced velocity, U^* (vertical lines) or the product of the reduced mass and the damping ratio, ζm^*; the circle ($A^* = 2, \zeta m^* = 1$) represents the reference configuration selected to compare the efficiency of different galloping bluff bodies (Fig. 4)

the maximum position is obtained by differentiation of Eq. (7), and ζm^* does not have an influence. The maximum efficiency grows as the parameter ζm^* grows [as deduced from Eq. (10)], and similar conclusions can be obtained by considering any other order of the parameters involved. The reference configuration ($A^* = 2, \zeta m^* = 1$) used to calculate the maximum efficiency of the different bluff bodies is represented by a circle in Fig. 5.

By keeping in mind Eqs. (7) and (10), each geometrical configuration can be represented by a single point if the self-similar variables A^*/U^* and $\eta_{max}U^*/(2\zeta m^*)$ are used instead of A^* and η_{max}. In these self-similar variables, Fig. 5 reduces to $A^*/U^* = 0.77$ and $\eta_{max}U^*/(2\zeta m^*) = 0.35$.

The values of the self-similar variables change with the body shape, but it is remarkable that, within the validity range of this simplified model, the transverse galloping energy harvesting properties of a given two-dimensional body can be summarized in a single point in the A^*/U^* versus $\eta_{max}U^*/(2\zeta m^*)$ plane.

Concerning Fig. 4, in the case of triangular cross-section prisms, which are identified by the angle β of the main vertex, $\tan\beta = b_m/(2c)$, there are several instable regions in the α_0-β plane (Alonso et al. 2005, 2007, 2009, 2010, 2012; Alonso and Meseguer 2006; Iungo and Buresti 2009). One of these regions is in the vicinity of $\alpha_0 = 180°$, whereas another one appears at approximately $\alpha_0 = 60°$. Obviously, to obtain energy from the galloping oscillations, the body under consideration must undergo instability, which means that at least the Glauert-Den Hartog criterion must be satisfied. Taking this fact into consideration, only those configurations that clearly meet this criterion ($\alpha_0 \cong 180°$) have been considered in Fig. 4.

According to Fig. 4, triangular cross-section bodies at $\alpha_0 = 180°$ seem to be the more promising ones for energy harvesting from the galloping phenomenon.

Conclusions

An improved approach to estimate the energy harvesting efficiency from the transverse galloping of bluff bodies using experimental data has been presented. The importance of properly choosing the process of fitting the polynomial curve of the aerodynamic force coefficient to the experimental set of data has been demonstrated with existing experimental data from bodies with different cross sections and with data obtained from new experiments. It has been proven that, unless the aerodynamic force coefficient experimental curve is extremely simple, experimental data cannot be fitted by a cubic polynomial, and higher powered terms must be retained in the series expansion (3) to reproduce the real behavior.

The inappropriate election of the polynomial used to fit the experimental data would give an unrealistic and an even too optimistic capability of the given body to gather energy from wind flow, or, in contrast, lead to disregarding the given two-dimensional body shape. This is based on a wrong estimation of the energy harvesting capability, which seems to be the case of isosceles triangular cross-section bodies in Barrero-Gil et al. (2010).

Another important conclusion is that, although there are many cross-section shapes that show transverse galloping instability in a range of angles of attack α_0, from the point of view of energy harvesting, only a few of them seem to be appropriate to give reasonable values of the maximum efficiency associated with the extraction of energy from the incident wind. Values of the maximum efficiency of different families of prisms are provided and compared. The most promising configuration seems to correspond to the reverse triangular cross-section prisms, and if the study is confined to isosceles triangles (identified by the angle β of the main vertex), the maximum efficiency is reached for triangles with a vertex angle close to $\beta = 60°$.

Further experimental investigations concerning triangular bodies (Ibarra et al. 2014) demonstrated that inverted isosceles triangles develop galloping instabilities at $U^* \cong 35$; in the case of isosceles

triangles with a main vertex $\beta = 60°$, where U^* stands for the reduced velocity, $U^* = U/(\omega_n c)$, where U is the air speed, ω_n is the first natural body frequency, and c is a characteristic length. Before galloping occurs, at lower wind velocities, $U^* \cong 3$, a vortex-induced vibration (VIV) episode appears. However, this VIV episode is of less interest from the point of view of wind energy harvesting, because VIV takes place at low air velocity (thus, the wind energy to be gathered is small) and because of the small amplitude of the body oscillations.

In galloping oscillations, these two effects are enlarged. In the experiments reported by Ibarra et al. (2014), the galloping phenomenon appears for $U^* > 35$, whereas VIV oscillations occur at $U^* \cong 3$, as already stated, which implies the galloping wind kinetic energy is more than 100 times greater than the one associated with vortex shedding. The oscillation amplitudes are highly dissimilar, and the ratio between galloping amplitude oscillation, A_G, and vortex-induced one, A_V, can be up to $A_G/A_V \geq 4$. In galloping experimentation, the allowed maximum oscillation amplitudes must be limited, and the experimental sequences should be stopped when such maxima of the oscillation amplitudes are reached, to avoid any damage to the setup.

From a practical point of view, the advantages of energy harvesting by using inverted isosceles triangles are probably limited by the drawbacks of large amplitude oscillations and the potential destructive effects of galloping instabilities, but the aspects of these problems are out of the scope of this paper.

References

Abdelkefi, A., Hajj, M. R., and Nayfeh, A. H. (2012a). "Power harvesting from transverse galloping of square cylinder." *Nonlinear Dyn.*, 70(2), 1355–1363.

Abdelkefi, A., Hajj, M. R., and Nayfeh, A. H. (2012b). "Phenomena and modeling of piezoelectric energy harvesting from freely oscillating cylinders." *Nonlinear Dyn.*, 70(2), 1377–1388.

Abdelkefi, A., Hajj, M. R., and Nayfeh, A. H. (2012c). "Modeling and analysis of piezoaeroelastic energy harvesters." *Nonlinear Dyn.*, 67(2), 925–939.

Abdelkefi, A., Hajj, M. R., and Nayfeh, A. H., (2013a). "Piezoelectric energy harvesting from transverse galloping of bluff bodies." *Smart Mater. Struct.*, 22(1), 015014.

Abdelkefi, A., Nayfeh, A. H., and Hajj, M. R. (2012d). "Design of piezoaeroelastic energy harvesters." *Nonlinear Dyn.*, 68(4), 519–530.

Abdelkefi, A., and Nuhait, A. O. (2013). "Modeling and performance analysis of cambered wing-based piezoaeroelastic energy harvesters." *Smart Mater. Struct.*, 22(9), 095029,

Abdelkefi, A., Scanlon, J. M., McDowell, E., and Hajj, M. R. (2013b). "Performance enhancement of piezoelectric energy harvesters from wake galloping." *Appl. Phys. Lett.*, 103, 033903.

Abdelkefi, A., Yan, Z., and Hajj, M. R. (2013c). "Modeling and nonlinear analysis of piezoelectric energy harvesting from transverse galloping." *Smart Mater. Struct.*, 22(2), 025016.

Abdelkefi, A., Yan, Z., and Hajj, M. R. (2014). "Performance analysis of galloping-based piezoaeroelastic energy harvesters with different cross-section geometries." *J. Intell. Mater. Syst. Struct.*, 25(2), 246–256.

Akaydin, H. D., Elvin, N., and Andreopoulos, Y. (2010). "Wake of a cylinder: A paradigm for energy harvesting with piezoelectric materials." *Exp. Fluids*, 49(1), 291–304.

Alonso, G., and Meseguer, J. (2006). "A parametric study of the galloping instability of two-dimensional triangular cross-section bodies." *J. Wind Eng. Ind. Aerodyn.*, 94(4), 241–253.

Alonso, G., and Meseguer, J. (2014). "Hysteresis phenomena in aerodynamics." *Hysteresis: Types, applications and behavior patterns in complex systems*, J. C. Dias, ed., Nova Science Publishers, Hauppauge, NY.

Alonso, G., Meseguer, J., and Pérez-Grande, I. (2005). "Galloping oscillations of two-dimensional triangular cross-sectional bodies." *Exp. Fluids*, 38(6), 789–795.

Alonso, G., Meseguer, J., and Pérez-Grande, I. (2007). "Galloping stability of triangular cross-sectional bodies: A systematic approach." *J. Wind Eng. Ind. Aerodyn.*, 95(9–11), 928–940.

Alonso, G., Meseguer, J., Sanz-Andrés, A., and Valero, E. (2010). "On the galloping instability of two-dimensional bodies having elliptical cross-sections." *J. Wind Eng. Ind. Aerodyn.*, 98(8–9), 438–448.

Alonso, G., Sanz-Lobera, A., and Meseguer, J. (2012). "Hysteresis phenomena in transverse galloping of triangular cross-section bodies." *J. Fluids Struct.*, 33, 243–251.

Alonso, G., Valero, E., and Meseguer, J. (2009). "An analysis on the dependence on cross section geometry of galloping stability of two-dimensional bodies having either biconvex or rhomboidal cross sections." *Eur. J. Mech. B/Fluids*, 28(2), 328–334.

Bae, J. S., and Inman, D. J. (2014). "Aeroelastic characteristics of linear and nonlinear piezo-aeroelastic energy harvester." *J. Intell. Mater. Syst. Struct.*, 25(4), 401–416.

Barrero-Gil, A., Alonso, G., and Sanz-Andrés, A. (2010). "Energy harvesting from transverse galloping." *J. Sound Vibrat.*, 329(14), 2873–2883.

Bryant, M., Wolff, E., and Garcia, E. (2011). "Aeroelastic flutter energy harvester design: The sensitivity of the driving instability to system parameters." *Smart Mater. Struct.*, 20(12), 125017.

Den Hartog, J. P. (1965). *Mechanical vibrations*, 4th Ed., McGraw Hill, New York.

Doaré, A., and Michelin, S. (2011). "Piezoelectric coupling in energy-harvesting fluttering flexible plates: Linear stability analysis and conversion efficiency." *J. Fluids Struct.*, 27(8), 1357–1375.

Erturk, A., Vieira, W. G. R., De Marqui C., Jr, and Inman, D. J. (2010). "On the energy harvesting potential of piezoaeroelastic systems." *Appl. Phys. Lett.*, 96, 184103.

Glauert, H. (1919). "The rotation of an aerofoil about a fixed axis." *(British) Advisory Committee for Aeronautics (ARC) R & M No. 595, Tech. Rep. of ARC for 1918–1919*, His Majesty's Stationery Office, London, 443–447.

Grouthier, C., Michelin, S., and de Langre, E. (2012). "Energy harvesting using vortex-induced vibrations of tensioned cables."

Hobbs, W. B., and Hu, D. L. (2012). "Tree-inspired piezoelectric energy harvesting." *J. Fluids Structures*, 28, 103–114.

Ibarra, D., Sorribes, F., Alonso, G., and Meseguer, J. (2014). "Transverse galloping of two-dimensional bodies having a rhombic cross-section." *J. Sound Vibrat.*, 333(13), 2855–2865.

Iungo, G. V., and Buresti, G. (2009). "Experimental investigation on the aerodynamic loads and wake flow features of low aspect-ratio triangular prisms at different wind directions." *J. Fluids Struct.*, 25(7), 1119–1135.

Jung, H.-J., and Lee, S. W. (2011). "The experimental validation of a new energy harvesting system based on the wake galloping phenomenon." *Smart Mater. Struct.*, 20(5), 055022.

Jung, H.-J., Lee, S. W., and Jang, D. D. (2009). "Feasibility study on a new energy harvesting electromagnetic device using aerodynamic instability." *IEEE Trans. Magn.*, 45(10), 4376–4379.

Luo, S. C., Chew, Y. T., Lee, T. S., and Yazdani, M. G. (1998). "Stability to translational galloping vibration of cylinders at different mean angles of attack." *J. Sound Vibrat.*, 215(5), 1183–1194.

Mackowski, A. W., and Williamson, C. H. K. (2013). "An experimental investigation of vortex-induced vibration with nonlinear restoring forces." *Phys. Fluids*, 25, 087101.

Mehmood, A., Abdelkefi, A., Hajj, M. R., Nayfeh, A. H., Akhtar, I., and Nuhait, A. O. (2013). "Piezoelectric energy harvesting from vortex-induced vibrations of circular cylinder." *J. Sound Vibrat.*, 332(19), 4656–4667.

Naudascher, E., and Rockwell, D. (1994). *Flow induced vibrations—An engineering guide*, A. A. Balkema, Rotterdam, Netherlands.

Ng, Y. T., Luo, S. C., and Chew, Y. T. (2005). "On using high-order polynomial curve fits in the quasi-steady theory for square-cylinder galloping." *J. Fluids Struct.*, 20(1), 141–146.

Novak, M. (1969). "Aeroelastic galloping of prismatic bodies." *J. Engrg. Mech. Div.*, 96, 115–142.

Novak, M. (1972). "Galloping oscillations of prismatic structures." *J. Engrg. Mech. Div.*, 98, 27–46.

Novak, M., and Tanaka, H. (1974). "Effect of turbulence on galloping instability." *J. Engrg. Mech. Div.*, 100, 27–47.

Païdoussis, M., Price, S., and de Langre, E. (2011). *Fluid–structure interactions: Cross-flow-induced instabilities*, Cambridge University Press, Cambridge, U.K., 15–104.

Peng, J., and Chen, G. S. (2012). "Flow-oscillating structure interactions and the applications to propulsion and energy harvest." *Appl. Phys. Res.*, 4(2).

Peng, Z., and Zhu, Q. (2009). "Energy harvesting through flow-induced oscillations of a foil." *Phys. Fluids*, 21, 123602.

Sewatkar, C. M., Sharma, A., and Agrawal, A. (2012). "On energy transfer in flow around a row of transversely oscillating square cylinders at low Reynolds number." *J. Fluids Struct.*, 31, 1–17.

Sirohi, J., and Mahadik, R. (2011). "Piezoelectric wind energy harvester for low-power sensors." *J. Intell. Mater. Syst. Struct.*, 22(18), 2215–2228.

Sirohi, J., and Mahadik, R. (2012). "Harvesting wind energy using a galloping piezoelectric beam." *J. Vib. Acoust.*, 134, 011009.

St. Clair, D., Bibo, A., Sennakesavababu, V. R., Daqaq, M. F., and Li, G. (2010). "A scalable concept for micropower generation using flow-induced self-excited oscillations." *Appl. Phys. Lett.*, 96, 144103.

Tang, L., Païdoussis, P., and Jang, J. (2009). "Cantilevered flexible plates in axial flow: Energy transfer and the concept of flutter-mill." *J. Sound Vibrat.*, 326(1–2), 263–276.

Wu, X., Ge, F., and Hong, Y. (2012). "A review of recent studies on vortex-induced vibrations of long slender cylinders." *J. Fluids Struct.*, 28, 292–308.

Zhao, L., Tang, L., and Yang, Y. 2012. "Small wind energy harvesting from galloping using piezoelectric materials." *ASME 2012 Conf. on Smart Materials, Adaptive Structures and Intelligent Systems*, ASME, New York, 919–927.

Zhu, Q. (2011). "Optimal frequency for flow energy harvesting of a flapping foil." *J. Fluid Mech.*, 675, 495–517.

Zhu, Q., Haase, M., and Wu, C. H. (2009). "Modeling the capacity of a novel flow-energy harvester." *Appl. Math. Modell.*, 33(5), 2207–2217.

AUTHOR QUERIES

AUTHOR PLEASE ANSWER ALL QUERIES

Q: A_NEW! ASCE Open Access: Authors may choose to publish their papers through ASCE Open Access, making the paper freely available to all readers via the ASCE Library website. ASCE Open Access papers will be published under the Creative Commons—Attribution Only (CC-BY) License. The fee for this service is $1750, and must be paid prior to publication. If you indicate Yes, you will receive a follow-up message with payment instructions. If you indicate No, your paper will be published in the typical subscribed-access section of the Journal.

Q: 1_Please check that ASCE Membership Grades (Member ASCE, Fellow ASCE, etc.) are provided for all authors who are members.

Q: 2_Per journal style, please provide the complete names for ''IDR/UPM'' and ''E.T.S.I.'' (These will also be expanded at first instance in the article, per style.)

Q: 3_In the equation ''d(α)...,'' the ''d'' is *italic*, while the ''d's'' used previously are roman; please confirm, throughout the article, whether ''*d*'' should instead be ''d''.

Q: 4_In Eq. (4) and subsequent equations, the asterisk (*) has been set as a superscript; please confirm or correct.

Q: 5_Per journal style, there may not be a single subhead in a section; please add at least one subhead to this ''Mathematical Model'' section, or delete this subhead.

Q: 6_Please clarify if this (3) refers to Eq. (3) or to the numbered list above this section.

Q: 7_The sentence beginning ''The fitting process is affected...'' was edited for readability; please confirm that it retains intended meaning.

Q: 8_Per style, all materials and equipment mentioned in the article must be identified by the manufacturer's name and location; please confirm/correct ATI DELTA.

Q: 9_Are changes to the sentence ''A close look at the curves...'' okay?

Q: 10_Please clarify if ''(3)'' refers to point 3 in the numbered list or to Equation (3).

Q: 11_For Grouthier et al. (2012), please confirm whether this article was published in print, as well as online; if in print, please provide complete citation.

Q: 12_For Peng and Chen (2012), please provide complete page range.

Q: 13_Reference ''Wu, Ge, Hong, 2012'' is not cited in the text. Please add an in-text citation or delete the reference.

Q: 14_In Fig. 1, the list of variables has been alphabetized per journal style; please confirm/correct.

Q: 15_Because Fig. 4 will print in black and white; ''black circles'' has been changed to ''solid circles'' to differentiate from the green-outlined circles—green-outlined circles will print in shades of gray.

Q: 16_Please add brief explanation stating how Fig. 4 is related to Fig. 5, as was done in Fig. 4 (i.e., ''prisms shown in Fig. 3'').

Q: 17_The original Table title for Table 1 was too long; the text has been added as a table footnote; please confirm that this does not alter intended meaning.

Q: 18_Column header changed from ''$\boldsymbol{A_1}$'' to ''$\boldsymbol{a_1}$,'' per table title; please confirm or correct.

Q: 19_Païdoussis et al. 2010 is not included in the reference list; please correct or delete the in-text citation.

Q: 20_Païdoussis et al. 2011 is not mentioned in the article text; please correct or delete this reference.